ACS OMEGA

Article

Cite This: ACS Omega 2018, 3, 15407−15415

http://pubs.acs.org/journal/acsodf

# Looking into Limoncello: The Structure of the Italian Liquor Revealed by Small-Angle Neutron Scattering

Leonardo Chiappisi*[,†,‡] and Isabelle Grillo[‡]

[†]Stranski Laboratorium für Physikalische Chemie und Theoretische Chemie, Institut für Chemie, Technische Universität Berlin, Strasse des 17. Juni 124, Sekr. TC7, , D-10623 Berlin, Germany

[‡]Institut Max von Laue−Paul Langevin, 71 avenue des Martyrs, 38042 Grenoble Cedex 9, France

Supporting Information

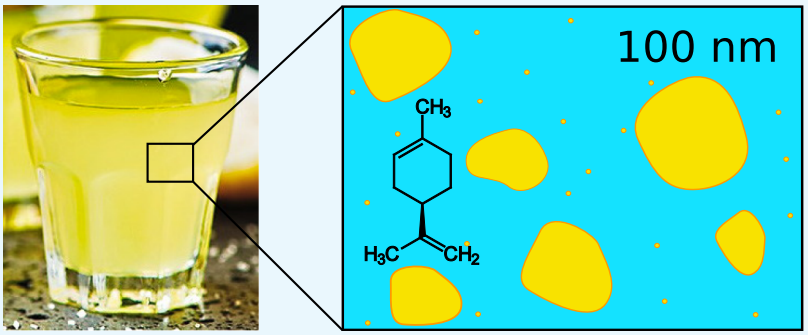


**ABSTRACT:** Limoncello, the Italian liquor based on lemon essential oils, is becoming increasingly popular around the world. This digestive is not only an iconic representative of Italian food culture, but it is also a complex colloidal system, made of essential oils, ethanol, sucrose, and water. Smell, aroma, taste, and appearance of Limoncello do, of course, depend on the components, in particular on the peculiar essential oil mixture. Accordingly, several studies are available in the literature investigating the composition of various Limoncellos. However, the microscopic structure plays an equally important role when it comes to the sensory properties of food and beverages. In this work, small-angle neutron scattering was used to probe the microscopic structure of Limoncello, revealing the presence of spontaneously formed 100 nm-sized droplets over a large range of composition and temperature. The results are not limited to this famous drink but can be extended to the rapidly developing formulations based on water-insoluble oils, water, and alcohols.

## INTRODUCTION

It is no exaggeration to say that almost every festive meal in southern Italy is crowned with a frozen glass of Limoncello, the famous Italian liquor renowned for its flavor and neon-yellow color. The traditional recipe foresees that the citrus zest, obtained by scraping the outer part of the lemon peels, is kept macerating in 95% vol ethanol for several (4−8) weeks. The zest, or flavedo, contains most of the essential oils giving rise to the characteristic taste and color of the liquor. The ethanolic extract is then filtered and diluted with a sucrose/water syrup previously prepared. Usually, the liquor contains ca. 30% vol of alcohol and ca. 20% vol of sucrose. However, the preparation procedure and exact final composition vary from family to family. Limoncello is also largely produced on an industrial scale, with an estimate of 15 million liters commercialized in 2003.[1] Three million liters were produced using the IGP lemon of Sorrento in 2017, according to the local consortium.

To assess the genuineness and quality of commercial Limoncellos, several analytical procedures have been developed.[1−5] Different studies performed on commercial Limoncellos reveal that, in several cases, the final product has never been in direct contact with the lemon peel, but it is rather a mixture of citrus essential oils, alcohol, water, and sucrose.[2,4] Multiple reasons are found for the rare employment of the traditional and time-consuming procedure, in addition to the obvious economic aspect. The composition of the lemon essential oil, extracted from the citrus flavedo, can vary significantly as a function of the harvest period and the growth location,[6] making a production of the liquor with constant organoleptic properties difficult. Moreover, Crupi et al. found evidence that commercial liquors were prepared using terpeneless oils or essential oils enriched with citral,[4] possibly to avoid or reduce oxidative processes and to enhance the liquor flavor and shelf-life.

In this work, the focus is put on the microscopic structure of Limoncello, rather than on its chemical composition. While the chemical composition is essentially determining the flavor of liquor, the microstructure of food and beverages strongly affects the sensory perception during tasting, on its shelf-life, and on the optical appearance.[7−12] From a physicochemical

Received: August 1, 2018
Accepted: October 29, 2018
Published: November 13, 2018




DOI: 10.1021/acsomega.8b01858
ACS Omega 2018, 3, 15407−15415

perspective, the Limoncello is a mixture of hydrophobic essential oils extracted from the lemon flavedo, ethanol, water, and sucrose. Similar ternary, or pseudo-ternary mixtures, formed by two partly miscible liquids (the water/sucrose syrup and the essential oil) and a common solvent, such as ethanol, exhibit strong composition fluctuations close to the phase-separation boundary,[13−17] that is, the mixtures become inhomogeneous both at the microscopic and macroscopic level, thus turning often turbid. This effect is commonly observed upon water addition to anise-flavored spirits, such as pastis, absinthe, raki, or ouzo, hence the name of "ouzo-effect".[18] Furthermore, the effect is not limited to alcoholic beverages, it is also exploited for the development of reaction media and promising drug delivery systems.[19−22] The size of the clusters strongly depends on the composition of the mixture and varies between a few nanometers in the so-called pre-ouzo region (thermodynamically stable and transparent) to micrometer-sized domains which exhibit slow phase separation in the ouzo region. It is noteworthy that there exists different designations in the literature to describe these systems, the two most common being surfactant-free emulsions, to distinguish them from the conventional cases of two immiscible liquids stabilized by surfactant molecules[20,23] or ultraflexible microemulsions, to highlight the exceptionally low rigidity of the droplet interface.[24,25]

The characterization of the microstructure of Limoncello was performed using small-angle neutron scattering (SANS), a very powerful technique for studying the structure of soft condensed matter in the range of Å ($10^{-10}$ m) to $\mu$m ($10^{-6}$ m), which was already successfully employed in similar ouzo-systems.[21,25,26] However, because of the high complexity of real food products, the use of scattering techniques is mostly limited to simplified, abstracted representations thereof.[27−30] In this study, the microstructure of "real" Limoncello samples made following a traditional receipt (apart from the use of deuterated compounds) is probed and compared to a model system comprising pure citrus essential oils. Isotopic labeling is a prerequisite for several techniques used in colloidal science, such as neutron scattering or nuclear magnetic resonance, and the effect of deuteration on the physicochemical properties of emulsion systems was investigated before.[31,32] While phase boundaries are slightly affected by the isotopic labeling, negligible effects on the emulsion morphology, that is, average size and size distribution, have been reported.[31,32]

## RESULTS

Before the small-angle scattering data can be analyzed and interpreted, the composition of the ethanolic extract has to be accessed. The essential oil extracted from citrus flavedo has a complex composition, and more than 60 volatile compounds have been identified.[4] The main components of the essential oil are monoterpenes, oxygenated compounds such as aldehydes, and sesquiterpenes.[1,3,4,33] Monoterpenes constitute 90% wt of the mixtures and are the main components of the citrus essential oil, with the most representative compounds being limonene, $\beta$-pinene, and $\gamma$-terpinene. Oxygenated compounds, such as decanal, geranial and neral—two isomers of citral—make up to 10% of the mixture. Sesquiterpenes, such as $\beta$-bisabolene, constitute ca. 1% of the essential oil mixture.

The amount of essential oil in the ethanolic extract was evaluated by proton nuclear magnetic resonance, $^1$H NMR (see the spectrum in Figure 1). A quantitative analysis was performed using tetramethylsilane (TMS) as an internal

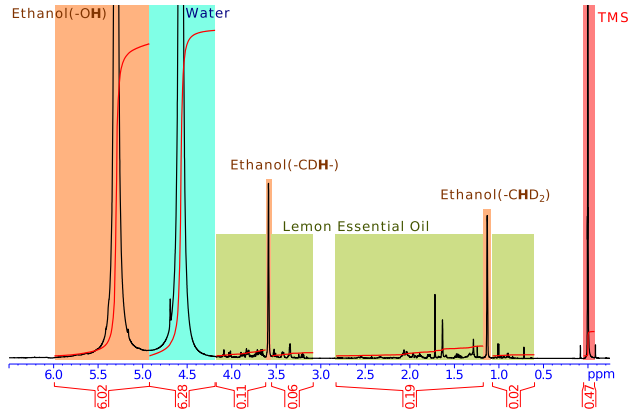


**Figure 1.** $^1$H NMR spectrum of the ethanolic extract to which a small aliquot of TMS was added.

standard. Different intense peaks are observed: one at 0 ppm of the internal reference TMS; two broad peaks centered at 4.6 and 5.3 ppm, which are ascribed to the water proton and to the hydroxyl proton of ethanol, respectively;[34,35] two singlets at 1.1 and 3.6 ppm, ascribed to residual light hydrogen of the ethanol (see the $^1$H NMR spectrum of deuterated ethanol in the Supporting Information); finally, a large number of peaks between 3.0 and 4.0 ppm and between 0.5 and 2.5 ppm, ascribed to the main components of the essential oil, are found.[36,37] Accordingly, the amount of "essential-oil-protons" can be estimated by the integral over these two regions, and the oil content in the ethanolic extract estimated assuming a generic chemical formula of $C_xH_{1.6x}$, typical of terpenes. With this assumption, an oil content in the extract of ca. 0.28% wt is estimated. Moreover, from the integrals of the two broad peaks at 4.6 and 5.3 ppm, the water content in the extract is estimated at 15% wt, in good agreement with the weight loss of the lemon peel after infusion in alcohol and with literature data.[38] It has to be remarked that the $^1$H NMR spectrum provides only an estimate of the amount of solubilized oil in the complex mixture, for example, the alkene hydrogens are buried under the large signal from hydroxylic groups.

Once the chemical composition of the ethanolic extract was identified, the mesoscopic structure of mixtures formed by the lemon essential oil, water, ethanol, and sucrose was studied by SANS. Samples along the dilution line of the ethanolic extract with the water/syrup were prepared (LM1 to LM5); the effect of the sucrose content in the liquor was also probed by preparing samples with constant ethanol/oil content and with variable water and sucrose amounts (LM5 to LM9). The location of the investigated samples within the pseudo-ternary phase diagram is shown in Figure 2. Furthermore, the effect of temperature within the range of 266 K (−7 °C) to 298 K (25 °C) was studied, to evaluate potential structural changes during consumption: from the chilled glass to our warm mouth. The ternary phase diagram water/ethanol/lemon essential oil is presented in Figure 2 and the phase diagram syrup/ethanol/lemon essential oil is provided in Figure S6 in the Supporting Information. Both phase diagrams are almost identical and in very close agreement with the phase diagram obtained with the pure limonene.[39] The very large two-phase domain is due to the poor solubility of limonene in water (0.01 g/L). The samples are prepared in the water-rich part of the phase diagram and contained less than 0.3% in mass of lemon oil.



DOI: 10.1021/acsomega.8b01858
ACS Omega 2018, 3, 15407−15415

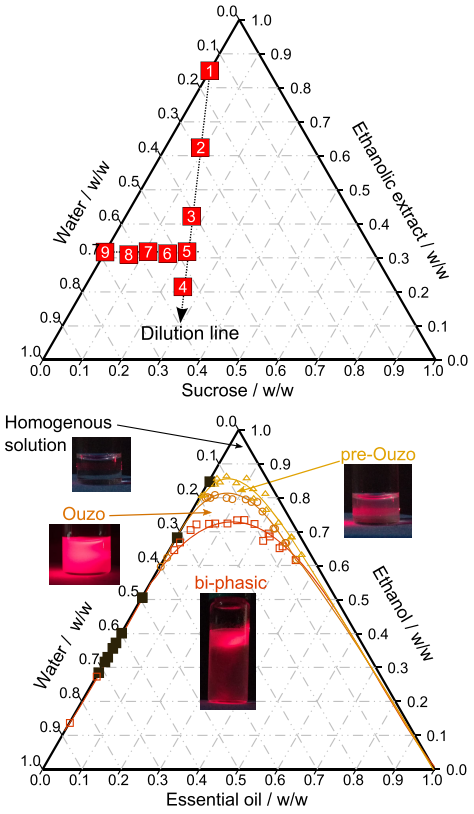


**Figure 2.** On the top, the ternary diagram reporting the composition of the samples used for the SANS analysis is given. The axes report the relative concentration of water, sucrose, and ethanol/essential oil mixture (∼ 0.3 %wt essential oil in $d_6$-ethanol). The number within the red square indicates the sample name and the position of the square its composition. Samples 1 to 5 were prepared by dilution of the ethanolic extract with the sucrose syrup; for samples 5 to 9 the amount of sucrose is systematically varied. See experimental section for further details. On the bottom, the phase diagram recorded for mixtures of water, ethanol, and a commercial citrus lemon essential oil extract is given; triangles represent the transition from the homogeneous to the pre-Ouzo region, circles represent the transition to the Ouzo-region, and squares delimit the region where rapid phase separation occurs. Concentrations are given in weight fraction. Lines are only a guide to the eyes. For the sake of comparison, the samples used for the SANS analysis, are also illustrated as dark squares. These points are compressed onto the left border due to the overall very low content of essential oil in the extract. Pictures of samples prepared in the four regions of the phase diagrams were taken under laser irradiation (633 nm, <1 mW) to highlight the turbidity of the sample.

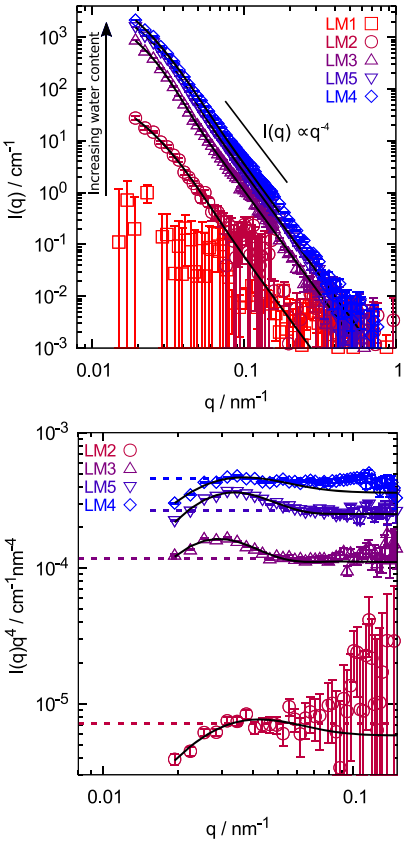


**Figure 3.** SANS patterns arising from ternary systems prepared by the dilution of the ethanolic extract with a water/sucrose syrup recorded at 298 K. On the top, the coherent scattering intensity is given as a function of the scattering vector. On the bottom, the scattering intensity multiplied with the fourth power of the scattering vector is given. The constant trend represents the Porod region, and the dotted lines indicate the Porod constant. The exact sample composition is given in Table 1 and their location in the pseudo-ternary diagram in Figure 2.

A representative set of SANS curves is given in Figure 3, where the scattering intensity $I(q)$ is plotted as a function of the scattering vector $q$. All other recorded patterns are given in the Supporting Information. The ethanolic extract (sample LM1), located in the ethanol-rich corner of the phase diagram, is homogeneous at a molecular scale, as proven by the very weak scattering intensity. As expected, the scattering intensity increases over 4 orders of magnitude upon addition of water, as evidenced in the left-hand-side plot of Figure 3. All curves look qualitatively very similar, with the main feature being an extended $q^{-4}$ power-law, typical for two-domain systems with a sharp interface. Typical examples are emulsions, marble, alloys presenting precipitate formation, or foams.[29,40−42] The observed scattering arises from the variation of the atomic composition at the interface between the domains and the suspending medium. Performing a Porod analysis allows us to determine the specific amount of interface Σ present in the system[43]

$$\Sigma = \frac{1}{2\pi\Delta\rho^2} \lim_{q\to\infty} I(q)q^4 \quad (1)$$

where $\Delta\rho$ is the scattering length difference between the domains and the medium. In the approximation that the oil droplets are spherical, the specific interface is related to the Porod radius $R_P$

$$\Sigma = \frac{3\phi}{R_P} \quad (2)$$

with $\phi$ being the volume fraction of the droplets. For the calculation of $\Delta\rho$ and $\phi$, we assumed that the essential oil droplets are suspended in a water/ethanol/sucrose mixture (see the Supporting Information for details). The scattering curves, however, present more features than a simple $q^{-4}$ power law. In fact, an oscillation is visible in the low-$q$ part of the $I(q)q^4$ representation (right-hand-side plot of Figure 3). This oscillation arises from the finite size of the essential oil droplets. Accordingly, the whole scattering pattern was described with a polydisperse sphere model, given by the following expression



DOI: 10.1021/acsomega.8b01858
ACS Omega 2018, 3, 15407−15415

$$I(q) = \Delta\rho^2 \int_0^\infty {}^1N\mathrm{Pdf(r)}V(r)P(q, r)\mathrm{d}r \text{ with } P(q, r) = \left[3\frac{\sin qr - qr\cos qr}{(qr)^3}\right]^2 \quad (3)$$

with ${}^1N$ being the number of droplets per unit of volume and $P$ d$f(r)$ the probability density function describing the relative abundance of a droplet of radius $r$ and volume $V(r) = 4/3\pi r^3$. Herein, a lognormal distribution was chosen to describe the polydisperse sizes of the emulsion droplets.[18] The probability density function, defined by two parameters, $\mu$ and $\sigma$, is given by

$$\mathrm{Pdf(r)} = \frac{1}{r\sigma\sqrt{2\pi}} \exp\left[-\frac{(\ln r - \ln \mu)^2}{2\sigma^2}\right] \quad (4)$$

The main advantage of the use of a lognormal distribution for the description of SANS data from polydisperse systems is that negative values for the droplet radius are not allowed and that the function can be used without any need of introducing cut-offs.

In summary, there are two procedures to obtain the size of the lemon essential oil droplets in the Limoncello mixtures: in the former one, the size is deduced from the scattering at the oil/medium interface, assuming the oil is completely separated from the solution; in the latter one, the patterns are analyzed with a model of polydisperse spheres, whereby the parameters $\mu$ and $\sigma$ describing the size distribution and the droplet volume fraction $\phi$ are optimized. In the right-hand-side plot of Figure 3, the Porod constant is indicated with the dashed line, while the polydisperse sphere model is indicated by a full line. Further details, calculated curves, and the obtained parameters are given in the Supporting Information. The Porod radius, calculated with eq 2, can be directly compared to the ratio of the third and second moment of the size distribution obtained from the full SANS analysis, given by

$$R_\mathrm{p} \equiv \frac{\langle R^3\rangle}{\langle R^2\rangle} = \mu \exp(2.5\sigma^2) \quad (5)$$

The calculated radii are given in Figure 4 as a function of the water content, for all samples recorded at the different temperatures. The temperature-dependence of the volume fraction of the components and of the scattering contrast was taken into account (see the Supporting Information for full details). The results from the Porod analysis indicate that the total amount of interface in the systems increases with increasing water content, which results, within the assumption of full microphase-separation of the essential oil from the medium, in a decreasing radius of the droplets. In contrast, the full analysis of the scattering patterns indicates that the size of the droplets is rather constant of ca. 100 nm for all investigated samples, and that the volume fraction of the oil droplets increases with increasing water content (see Figure S14). Both analyses deliver the same, consistent results for the samples with the highest water content (>55% wt).

The discrepancy between the droplet sizes obtained from the Porod analysis and those obtained from the fit with a polydisperse sphere model indicates that, at low water content, a significant amount of essential oil is molecularly dissolved in the solution and is not participating in the formation of the emulsified droplets. A wrong assumption on the volume fraction of oil droplets leads therefore to an overestimation of

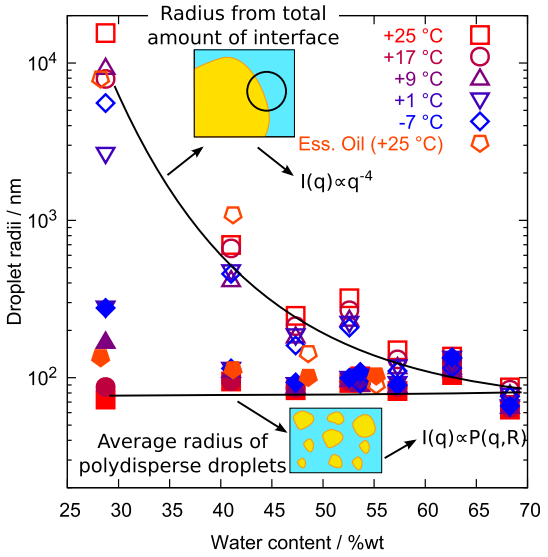


**Figure 4.** Average droplet size found in the different Limoncello samples by the analysis of the SANS patterns. Empty symbols represent sizes obtained via the Porod analysis (eqs 1 and 2) under the assumption that the essential oil completely separates into domains dispersed in the water/alcohol/sucrose mixture. Full symbols result from modeling the SANS curves with a polydisperse sphere model (eq 3), whereby the amount of separated oil was not fixed in the model. Full lines are only a guide for the eye. If a full microphase separation between the oil and the remaining components would take place, the two analyses would lead to the same results.

the Porod radius via eq 2. In fact, the sample LM1, with a water content as low as 15% wt, is a homogeneous solution, where all components are molecularly dissolved. Furthermore, the volume fraction of the oil droplets obtained from the polydisperse sphere model increases from less than 0.01% vol for the LM2 sample to ca. 0.15% vol (see Figure S16). The latter coincides with the predictions made from the ${}^1$H NMR results for the samples with the highest water content (LM8 and LM9).

It is worth mentioning that the analysis of the SANS data with the model of polydisperse sphere suffers from the lack of a clear plateau at low-$q$ values, which would clearly define the size of and the volume fraction of the spontaneously emulsified oil droplets. However, the latter can be evaluated in an independent fashion from the Porod integral[44,45]

$$Q^* = \int_0^\infty I(q)q^2\,\mathrm{d}q = 2\pi^2\Delta\rho^2\phi(1-\phi) \quad (6)$$

The obtained volume fractions of oil droplets are fully consistent with the values obtained from the fit of the data with the polydisperse sphere model (see Figure S17 in the Supporting Information). This consistency further corroborates the validity of the results from the polydisperse sphere model analysis.

The study also reveals that temperature does not affect the microstructure of the Limoncello in the studied temperature range (−7 to 25 °C), except that the solubility of the essential oil in the mixed solvent increases with increasing temperature, in agreement with previous studies on (+)limonene/water/ethanol mixtures.[46] Surprisingly, the presence of large amounts of sucrose, up to 25% wt, does not alter the microstructure of the Limoncello samples. This observation is further confirmed by the fact that the presence of sucrose minimally affects the



DOI: 10.1021/acsomega.8b01858
ACS Omega 2018, 3, 15407−15415

phase behavior of the mixtures of essential oil/ethanol/water, as shown in the Supporting Information in Figure S6.

The size of the self-emulsified oil domains is relatively small when compared to other ternary oil/water/ethanol mixtures, where typical sizes of larger than 500 nm are found.[25,29] The small size can be explained by the presence of surface active molecules, for example, lipids or proteins, extracted during the maceration of the lemon zest. It is likely that these components stabilize the oil/water interface leading to smaller oil droplets.[30,47] To verify this hypothesis, additional SANS experiments were performed on pseudo-Limoncello samples prepared by mixing water, sucrose, ethanol, and lemon essential oil, thus avoiding the direct contact of ethanol and the lemon zests during the maceration process. SANS patterns are shown in Figure 5. The data were recorded on an extended

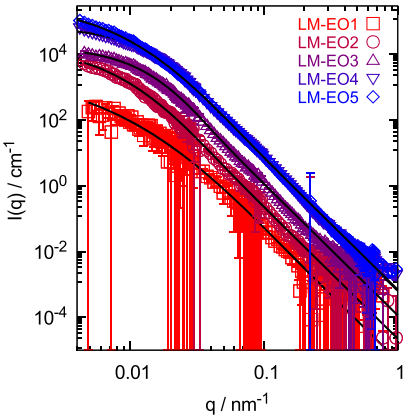


**Figure 5.** SANS patterns arising from ternary systems prepared from mixing cold-pressed essential lemon oil, ethanol, water, and sucrose and recorded at 298 K. The exact composition is given in Table 1.

$q$-range, thus covering also the Guinier region at low-$q$. They were analyzed with the same models described earlier in the text, the droplet radii are given in Figure 4 and show excellent agreement with the results from the "real" Limoncello samples. The finding rules out that the exceptionally small sizes found in these mixtures are caused by the presence of non-oily, surface-active components, such as lipids and proteins. In addition, the good agreement corroborates the correctness of the estimate of the essential oil content in the ethanolic extract used to prepare the "real" Limoncello samples and that the missing Guinier plateau does not lead to a misinterpretation of the scattering data.

Finally, the interfacial tension between lemon essential oil and water/sucrose/ethanol was determined by pending drop experiments. A low, but not extraordinary low, value of the interfacial tension of 4−5 mN/m (see the last paragraph of the Supporting Information) was found. Similar values were found between the oil-rich and oil-poor phase in water/ethanol/1-octanol mixtures.[13]

## DISCUSSION

The microstructure of the Limoncello samples prepared in this work is surprisingly stable. Except for the ethanolic extract, in all samples the presence of polydisperse essential oil droplets with an average size of ca. 100 nm is demonstrated. Neither the presence of sucrose nor changes in temperature have an effect on the microstructure of the investigated Limoncello samples. The size of the oil-domains of ca. 100 nm is surprisingly small when compared to the typical size of ouzo-systems which ranges from 500 nm to several micrometers.[25,29] The small size of the Limoncello droplets does not arise from the presence of surface-active contaminants, for example, lipids or proteins extracted during the maceration of the lemon zest. It is more likely that the complex mixture of the essential oil is able to stabilize droplets, whose size is intermediate between classical microemulsions (2−20 nm) and metastable ouzo-systems or classical oil/water emulsions (>500 nm).

While the size of the domains remains basically constant with temperature and composition, a continuous evolution in the amount of essential oil which participates in the droplet formation is observed. Sample LM1, with a water content of 15% wt (ethanol content of ca. 85% wt), is fully homogeneous, and no concentration fluctuations were observed. On the contrary, a complete microphase separation of the essential oils from the continuous phase is obtained for a water content larger than 60% wt. Interestingly, high-quality Limoncello samples have usually a composition close to the LM5 sample, with a water content of ca. 50% wt. At this composition, 1/3 of the essential oil is molecularly dispersed in the continuous phase (Figure S16). The microstructure of Limoncello is fundamental for the different properties of the liquor: the droplet size will affect the optical appearance and time-stability of the drink. Moreover, droplet size and distribution of the active fragrance within the mixture is expected to have a pronounced effect on the vapor pressure of the active perfume molecules, and therefore on the smell of the liquor. In a recent work, Zemb et al. have shown that the vapor pressure of a model fragrance, styrallyl acetate, dissolved in a water/ethanol mixture, reaches a maximum close to the boundary between the meta-stable ouzo region and the biphasic domain.[17] A lower activity of the fragrance is observed in the homogeneous region, where it is well-dissolved as well as in the biphasic domain, where the active components are trapped in micrometer sized droplets. Further studies evidenced that the solubilization of the fragrance in micellar aggregates reduces their evaporation rate,[48] in agreement with the finding that the evaporation of the active component from a surfactant stabilized air/water interface is limited by its diffusion through a depleted region close to the surface.[49] According to these findings, it seems that Limoncello samples with a composition close to LM5 present all the needed properties for a good digestive: the rather large fraction of free essential oils ensures a strong smell and taste of the liquor, which made it so popular. The typical droplet size of approx. 100 nm gives rise to the typical opalescent appearance but ensures both long-time stability and a rapid exchange between molecularly dissolved essential oil and small droplets. Noteworthy, a home-made Limoncello, prepared with hydrogenated water and ethanol close to the composition of LM5 and the same lemons of the experiment reported herein, had an excellent taste.

## CONCLUSIONS

In this work, a structural analysis of real Limoncello samples was performed using SANS, shedding light for the first time on the mesoscopic structure of this very famous Italian liquor. The results show that the system is composed of polydisperse oil droplets dispersed in a continuous water/ethanol/sucrose medium. These droplets, whose size of ca. 100 nm shows little variation with temperature and overall composition, are in equilibrium with molecularly dissolved essential oil. Interestingly, at a system composition close to that of commercial


DOI: 10.1021/acsomega.8b01858
ACS Omega 2018, 3, 15407−15415

Table 1. Composition of Samples Used in This Work[a]

| | weight fraction | | | | volume fraction at 298 K | | | |
|---|---|---|---|---|---|---|---|---|
| sample name | oil (%) | $d_6$-EtOH (%) | sucrose (%) | water (%) | oil (%) | EtOH (%) | sucrose (%) | water (%) |
| LM1 | 0.28 | 84.7 | 0.0 | 15.0 | 0.30 | 86.1 | 0.0 | 13.6 |
| LM2 | 0.21 | 62.2 | 8.9 | 28.7 | 0.24 | 67.9 | 5.4 | 26.4 |
| LM3 | 0.14 | 42.1 | 16.8 | 41.0 | 0.18 | 49.3 | 10.9 | 39.6 |
| LM4 | 0.07 | 21.4 | 24.9 | 53.6 | 0.10 | 27.0 | 17.5 | 55.4 |
| LM5 | 0.10 | 31.7 | 20.8 | 47.3 | 0.14 | 38.6 | 14.1 | 47.2 |
| LM6 | 0.10 | 31.2 | 16.1 | 52.6 | 0.15 | 37.5 | 10.8 | 51.7 |
| LM7 | 0.10 | 31.7 | 10.9 | 57.3 | 0.15 | 37.4 | 7.2 | 55.3 |
| LM8 | 0.10 | 30.9 | 6.4 | 62.6 | 0.15 | 36.0 | 4.1 | 59.7 |
| LM9 | 0.10 | 31.6 | 0.00 | 68.3 | 0.15 | 36.1 | 0.0 | 63.8 |
| LM-EO1 | 0.41 | 87.9 | 0.0 | 11.7 | 0.44 | 89.9 | 0.0 | 9.7 |
| LM-EO2 | 0.31 | 66.2 | 8.0 | 25.6 | 0.36 | 72.2 | 4.8 | 22.6 |
| LM-EO3 | 0.21 | 44.0 | 16.1 | 39.7 | 0.26 | 51.6 | 10.5 | 37.7 |
| LM-EO4 | 0.15 | 33.0 | 20.2 | 46.7 | 0.20 | 40.1 | 13.7 | 46.1 |
| LM-EO5 | 0.10 | 22.3 | 24.1 | 53.5 | 0.14 | 28.2 | 16.9 | 54.8 |

[a]LM*x* series are samples prepared from the ethanolic extract, and the amount of essential oil was evaluated from the $^1$H NMR spectrum shown in Figure 1. LM-EO*x* sample series denote samples prepared using cold-pressed lemon essential oil. The conversion from weight fractions to volume fractions was performed using the density values given in Table 2.

Limoncellos, ca. 1/3 of the essential oil is molecularly dissolved and in equilibrium with the sub-micrometer large droplets. It is expected that the overall sensory experience of Limoncello: its smell, taste, and optical appearance, results from this delicate equilibrium.

However, the relevance of the study goes beyond the use of neutron scattering for the characterization of a tasty digestive. Essential oils, especially limonene, are experiencing quickly growing applications. In addition to the traditional use as flavors and fragrances, the oils extracted from citrus fruits are becoming increasingly relevant, for example, as green solvents in replacement of petro-based chemicals for specific applications,[50−54] as speciality chemicals,[55−58] or as bio-based monomer or monomer precursors for polymerization reactions.[37,59,60] An increased use of essential oils has several implications, from an environmental and socio-economic perspective. The increasing demand for citrus essential oils induces the development of new industrial activities aiming at the treatment of citrus waste products thus reducing the environmental impact of direct landfilling of the citrus waste[50] and providing economic growth opportunities in the citrus-producing regions, such as Latin America, Southeast Asia, and Southern Europe. In particular, the potential of pseudo-ternary systems made of water/alcohol/essential oils is being currently explored, and recent developments are reported, for example, as mosquito-repellent formulations[61,62] or as a medium for enzymatic and chemical reactions.[20,22,63] To understand these systems, with the aim of tailoring them to the desired need, a detailed knowledge of the microscopic structure is mandatory, and, SANS provides a unique tool, as shown in this work for the case of Limoncello.

To conclude, the work reports the spontaneous formation of 100 nm-sized essential oil droplets in a continuous polar phase, which are stable over a long time range. These findings open two fundamental questions to be addresses in forthcoming studies: what are the physical forces leading to the formation of oil domains with such an exceptional size and what is the mechanism guaranteeing a long term stability to Limoncello systems.

## MATERIALS AND METHODS

**Materials and Sample Preparation.** The samples were prepared using deuterated water (*D* content >99.8%) from Eurisotop (Gif-sur-Yvette, France), $d_6$-ethanol (99% purity) from Deutero (Kastellaun, Germany), commercial sucrose, and nontreated lemons from Sicily bought at a local market. The ethanolic extract was prepared by immersing 2.5 g of the outer part of lemon skins, the flavedo, in 12.6 g of pure fully deuterated ethanol. The lemon peels were kept macerating in the absolute deuterated alcohol for 4 weeks. After this period, a sucrose syrup was prepared by dissolving 6.6 g of sucrose in 13.2 g of $D_2O$. Samples were prepared by addition of the syrup and/or $D_2O$ to the ethanolic extract. Gentle shaking is sufficient for homogenization. The final composition of the samples is given in Table 1. The composition of the ethanolic extract was determined via $^1$H NMR as described before. Further samples were prepared using cold-pressed lemon essential oil from Arkpharma (Carros, France).

**Phase Diagram Determination.** The phase diagrams were visually determined. Binary mixtures of cold-pressed lemon essential oil and ethanol at different ratios were prepared by weighing the proper amounts of chemicals in 5 mL glass tubes. Small amounts of water, or of a 33% wt sucrose solution, were added gradually. The binary essential oil/ethanol mixtures are perfectly transparent. The transition to the pre-ouzo region is identified as the first signs of opalescence are detected. Further addition of water, or of a 33% wt sucrose solution, causes the system to turn highly turbid. The transition from translucent to turbid delimits the metastable ouzo-region. In the oil-rich part, further addition of water induces a sudden phase separation of the sample corresponding to the binodal line. The 2-phase domain is more difficult to observe in the oil-poor domain, where the phase separation only appears after several hours at rest.

**Methods.** *Small-Angle Neutron Scattering.* SANS patterns were recorded on D11 at the Institut Laue−Langevin (ILL) in Grenoble, France.[64,65] Raw and reduced data are available at doi:10.5291/ILL−DATA.INTER−372. Three different configurations were used, with a wavelength of $\lambda$ = 6.0 Å, sample-to-detector distances (SD) of 1.2, 8, and 34 m and collimation of 4, 8, and 34 m, respectively, covering a *q*-



DOI: 10.1021/acsomega.8b01858
ACS Omega 2018, 3, 15407−15415

range of 0.015−5 $nm^{-1}$, where $q = 4\pi \sin(\theta/2)/\lambda$ is the magnitude of the scattering vector and $\theta$ is the scattering angle. An additional configuration was used for the samples prepared with cold-pressed lemon essential oil, with a sample-to-detector distance of 39 m, collimation of 40 m, wavelength $\lambda$ = 12 Å, and removing the beam-stop, reaching a minimum $q$ value of 0.004 $nm^{-1}$. The differential cross sections in absolute scale were obtained by comparison with the scattering from a 1 mm water sample. The analysis was performed using the values of densities and scattering length densities $\rho$ of the compounds reported in Table 2.

**Table 2. Density and Neutron Scattering Length Densities ($\rho$) at 298 K of the Components of the Mixtures Studied in This Work**[a]

| compound | chemical formula | density/g $cm^{-3}$ | $\rho/10^{-4}$ $nm^{-2}$ |
|---|---|---|---|
| light water | $H_2O$ | 1.0 | −0.56 |
| heavy water | $D_2O$ | 1.1 | 6.33 |
| $d_6$-ethanol | $C_2D_6O$ | 0.89 | 6.10 |
| sucrose (H) | $C_{12}H_{22}O_{11}$ | 1.6 | 1.7 |
| lemon essential oil (terpenes) | $C_xH_{1.6x}$ | 0.84 | 0.25 |

[a]Density values of limonene and sucrose in water/ethanol mixtures are taken from refs,[35,66] respectively.

*$^1H$ NMR.* $^1H$ NMR spectra were recorded on a 700 MHz Bruker AVANCE III HD spectrometer. Experiments were carried out at 25 °C.

*Interfacial Tension.* The interfacial tension between the citrus essential oil and the water/sucrose/ethanol solution was measured at room temperature using a drop shape analyzer DSA10 from Krüss. Drops of oil in heavy water were created using an inverted blunt needle of 0.72 mm in diameter immersed in a 10 mm (thickness) × 20 mm (width) × 40 mm (height) optical glass cuvette. The interfacial tension was calculated from the drop profile by the Krüss software using the Young−Laplace equation.

## ■ ASSOCIATED CONTENT

### Supporting Information

The Supporting Information is available free of charge on the ACS Publications website at DOI: 10.1021/acsomega.8b01858.

Additional sample characterization, further phase diagrams, further SANS patterns and their interpretation, and interfacial tension results (PDF)

## ■ AUTHOR INFORMATION


### Corresponding Author

*E-mail: leonardo.chiappisi@tu-berlin.de.

### ORCID

Leonardo Chiappisi: 0000-0002-4594-2865


### Notes

The authors declare no competing financial interest.

## ■ ACKNOWLEDGMENTS

We thank Sylvain Prévost for fruitful discussions, the partnership for soft condensed matter (PSCM) for providing the laboratory infrastructure, and the Institut Laue−Langevin (ILL) for the allocation of SANS beamtime. We thank Adrien Favier and Alicia Vallet, from the IBS platform of the Partnership for Structural Biology and the Institut de Biologie Structurale in Grenoble (PSB/IBS), for the NMR access and the support provided. L.C. acknowledges the TU-Berlin and the ILL for postdoctoral funding through a three-year cooperation agreement.

## ■ REFERENCES


(1) Andrea, V.; Nadia, N.; Teresa, R. M.; Andrea, A. Analysis of some Italian lemon liquors (Limoncello). *J. Agric. Food Chem.* **2003**, *51*, 4978−4983.

(2) Fasoli, E.; Colzani, M.; Aldini, G.; Citterio, A.; Righetti, P. G. Lemon peel and Limoncello liqueur: a proteomic duet. *Biochim. Biophys. Acta* **2013**, *1834*, 1484−1491.

(3) Mehl, F.; Marti, G.; Boccard, J.; Debrus, B.; Merle, P.; Delort, E.; Baroux, L.; Raymo, V.; Velazco, M. I.; Sommer, H.; Wolfender, J.-L.; Rudaz, S. Differentiation of lemon essential oil based on volatile and non-volatile fractions with various analytical techniques: A metabolomic approach. *Food Chem.* **2014**, *143*, 325−335.

(4) Crupi, M.; Costa, R.; Dugo, P.; Dugo, G.; Mondello, L. A comprehensive study on the chemical composition and aromatic characteristics of lemon liquor. *Food Chem.* **2007**, *105*, 771−783.

(5) Da Costa, N. C.; Anastasiou, T. J. Analysis of volatiles in Limoncello liqueur and aging study with sensory. *ACS Symp. Ser.* **2010**, *1036*, 177−193.

(6) Poiana, M.; Geraldina, A.; Donatella, A.; Marisa, D. M. Alcoholic Extracts Composition from Lemon Fruits of the Amalf-Sorrento Peninsula. *J. Essent. Oil Res.* **2006**, *18*, 432−437.

(7) Rao, J.; McClements, D. J. Impact of lemon oil composition on formation and stability of model food and beverage emulsions. *Food Chem.* **2012**, *134*, 749−757.

(8) Tadros, T.; Izquierdo, P.; Esquena, J.; Solans, C. Formation and stability of nano-emulsions. *Adv. Colloid Interface Sci.* **2004**, *108−109*, 303−318.

(9) Malone, M. E.; Appelqvist, I. A. M.; Norton, I. T. Oral behaviour of food hydrocolloids and emulsions. Part 2. Taste and aroma release. *Food Hydrocolloids* **2003**, *17*, 775−784.

(10) McClements, D. J. Edible nanoemulsions: fabrication, properties, and functional performance. *Soft Matter* **2011**, *7*, 2297−2316.

(11) Stieger, M.; van de Velde, F. Microstructure, texture and oral processing: New ways to reduce sugar and salt in foods. *Curr. Opin. Colloid Interface Sci.* **2013**, *18*, 334−348.

(12) Lett, A. M.; Yeomans, M. R.; Norton, I. T.; Norton, J. E. Enhancing expected food intake behaviour, hedonics and sensory characteristics of oil-in-water emulsion systems through microstructural properties, oil droplet size and flavour. *Food Qual. Prefer.* **2016**, *47*, 148−155.

(13) Zemb, T. N.; Klossek, M.; Lopian, T.; Marcus, J.; Schöettl, S.; Horinek, D.; Prevost, S. F.; Touraud, D.; Diat, O.; Marčelja, S.; Kunz, W. How to explain microemulsions formed by solvent mixtures without conventional surfactants. *Proc. Natl. Acad. Sci. U.S.A.* **2016**, *113*, 4260−4265.

(14) Marcus, J.; Touraud, D.; Prévost, S.; Diat, O.; Zemb, T.; Kunz, W. Influence of additives on the structure of surfactant-free microemulsions. *Phys. Chem. Chem. Phys.* **2015**, *17*, 32528−32538.

(15) Fischer, V.; Marcus, J.; Touraud, D.; Diat, O.; Kunz, W. Toward surfactant-free and water-free microemulsions. *J. Colloid Interface Sci.* **2015**, *453*, 186−193.

(16) Marcus, J.; Klossek, M. L.; Touraud, D.; Kunz, W. Nanodroplet formation in fragrance tinctures. *Flavour Fragrance J.* **2013**, *28*, 294−299.

(17) Tchakalova, V.; Zemb, T.; Benczédi, D. Evaporation triggered self-assembly in aqueous fragrance−ethanol mixtures and its impact on fragrance performance. *Colloids Surf., A* **2014**, *460*, 414−421.

(18) Vitale, S. A.; Katz, J. L. Liquid Droplet Dispersions Formed by Homogeneous Liquid−Liquid Nucleation: "The Ouzo Effect". *Langmuir* **2003**, *19*, 4105−4110.




DOI: 10.1021/acsomega.8b01858
*ACS Omega* 2018, 3, 15407−15415

(19) Lepeltier, E.; Bourgaux, C.; Couvreur, P. Nanoprecipitation and the "Ouzo effect": Application to drug delivery devices. *Adv. Drug Delivery Rev.* **2014**, *71*, 86−97.
(20) Hou, W.; Xu, J. Surfactant-free microemulsions. *Curr. Opin. Colloid Interface Sci.* **2016**, *25*, 67−74.
(21) Schöttl, S.; Horinek, D. Aggregation in detergent-free ternary mixtures with microemulsion-like properties. *Curr. Opin. Colloid Interface Sci.* **2016**, *22*, 8−13.
(22) Xenakis, A.; Zoumpanioti, M.; Stamatis, H. Enzymatic reactions in structured surfactant-free microemulsions. *Curr. Opin. Colloid Interface Sci.* **2016**, *22*, 41−45.
(23) Schöttl, S.; Horinek, D. Salt effects in surfactant-free microemulsions. *J. Chem. Phys.* **2018**, *148*, 222818.
(24) Prevost, S.; Lopian, T.; Pleines, M.; Diat, O.; Zemb, T. Small-angle scattering and morphologies of ultra-flexible microemulsions. *J. Appl. Crystallogr.* **2016**, *49*, 2063−2072.
(25) Prévost, S.; Gradzielski, M.; Zemb, T. Self-assembly, phase behaviour and structural behaviour as observed by scattering for classical and non-classical microemulsions. *Adv. Colloid Interface Sci.* **2017**, *247*, 374−396.
(26) Diat, O.; Klossek, M. L.; Touraud, D.; Deme, B.; Grillo, I.; Kunz, W.; Zemb, T. Octanol-rich and water-rich domains in dynamic equilibrium in the pre-ouzo region of ternary systems containing a hydrotrope. *J. Appl. Crystallogr.* **2013**, *46*, 1665−1669.
(27) Lopez-Rubio, A.; Gilbert, E. P. Neutron scattering: a natural tool for food science and technology research. *Trends Food Sci. Technol.* **2009**, *20*, 576−586.
(28) Ubbink, J.; Burbidge, A.; Mezzenga, R. Food structure and functionality: a soft matter perspective. *Soft Matter* **2008**, *4*, 1569.
(29) Grillo, I. Small-angle neutron scattering study of a world-wide known emulsion: Le Pastis. *Colloids Surf., A* **2003**, *225*, 153−160.
(30) Dave, H.; Gao, F.; Schultz, M.; Co, C. C. Phase behavior and SANS investigations of edible sugar−limonene microemulsions. *Colloids Surf., A* **2007**, *296*, 45−50.
(31) Huang, J. S.; Sung, J.; Wu, X.-L. The effect of H2O and D2O on a water-in-oil microemulsion. *J. Colloid Interface Sci.* **1989**, *132*, 34−42.
(32) Baglioni, P.; Dei, L.; Gambi, C. M. C. Hydrogen isotope substitution in a water-in-oil microemulsion: Quasi-elastic light scattering. *J. Phys. Chem.* **1995**, *99*, 5035−5039.
(33) Di Vaio, C.; Graziani, G.; Gaspari, A.; Scaglione, G.; Nocerino, S.; Ritieni, A. Essential oils content and antioxidant properties of peel ethanol extract in 18 lemon cultivars. *Sci. Hortic.* **2010**, *126*, 50−55.
(34) Mizuno, K.; Miyashita, Y.; Shindo, Y.; Ogawa, H. NMR and FT-IR Studies of Hydrogen Bonds in Ethanol−Water Mixtures. *J. Phys. Chem.* **1995**, *99*, 3225−3228.
(35) Ogawa, H.; Murase, N.; Murakami, S. Behavior of solutes in water + ethanol mixed solvent. Part 1. Partial molar volumes, enthalpies of solution and chemical shift of 1H NMR for sucrose, urea and 1-phenyl-2-thiourea solutes. *Thermochim. Acta* **1995**, *253*, 41−49.
(36) Mills, N. S. Complete Assignment of Proton Chemical Shifts in Terpenes: An Experiment Combining 2D NMR Spectroscopy with Molecular Modeling. *J. Chem. Educ.* **1996**, *73*, 1190.
(37) Crockett, M. P.; Evans, A. M.; Worthington, M. J. H.; Albuquerque, I. S.; Slattery, A. D.; Gibson, C. T.; Campbell, J. A.; Lewis, D. A.; Bernardes, G. J. L.; Chalker, J. M. Sulfur-Limonene Polysulfide: A Material Synthesized Entirely from Industrial By-Products and Its Use in Removing Toxic Metals from Water and Soil. *Angew. Chem., Int. Ed.* **2016**, *55*, 1714−1718.
(38) Naviglio, D.; Montesano, D.; Gallo, M. Laboratory production of lemon liqueur (Limoncello) by conventional maceration and a two-syringe system to illustrate rapid solid−liquid dynamic extraction. *J. Chem. Educ.* **2015**, *92*, 911−915.
(39) Buchecker, T.; Krickl, S.; Winkler, R.; Grillo, I.; Bauduin, P.; Touraud, D.; Pfitzner, A.; Kunz, W. The impact of the structuring of hydrotropes in water on the mesoscale solubilisation of a third hydrophobic component. *Phys. Chem. Chem. Phys.* **2017**, *19*, 1806−1816.
(40) Anovitz, L. M.; Lynn, G. W.; Cole, D. R.; Rother, G.; Allard, L. F.; Hamilton, W. A.; Porcar, L.; Kim, M.-H. A new approach to quantification of metamorphism using ultra-small and small angle neutron scattering. *Geochim. Cosmochim. Acta* **2009**, *73*, 7303−7324.
(41) Axelos, M. A. V.; Boué, F. Foams As Viewed by Small-Angle Neutron Scattering. *Langmuir* **2003**, *19*, 6598−6604.
(42) Panagos, P.; Wang, Y.; McCartney, D. G.; Li, M.; Ghaffari, B.; Zindel, J. W.; Miao, J.; Makineni, S.; Allison, J. E.; Shebanova, O.; Robson, J. D.; Lee, P. D. Characterising precipitate evolution in multi-component cast aluminium alloys using small-angle X-ray scattering. *J. Alloys Compd.* **2017**, *703*, 344−353.
(43) Porod, G. Die Abhängigkeit der Röntgenkleinwinkelstreuung von Form und Grösse der kolloiden Teilchen in verdünnten Systemen, IV. *Acta Phys. Austriaca* **1947**, *2*, 255−292.
(44) Berti, D.; Baldelli Bombelli, F.; Fortini, M.; Baglioni, P. Amphiphilic self-assemblies decorated by nucleobases. *J. Phys. Chem. B* **2007**, *111*, 11734−11744.
(45) Roger, K.; Botet, R.; Cabane, B. Coalescence of Repelling Colloidal Droplets: A Route to Monodisperse Populations. *Langmuir* **2013**, *29*, 5689−5700.
(46) Cháfer, A.; Muñoz, R.; Burguet, M. C.; Berna, A. The influence of the temperature on the liquid−liquid equlibria of the mixture limonene + ethanol + H2O. *Fluid Phase Equilib.* **2004**, *224*, 251−256.
(47) Rao, J.; McClements, D. J. Formation of flavor oil micro-emulsions, nanoemulsions and emulsions: Influence of composition and preparation method. *J. Agric. Food Chem.* **2011**, *59*, 5026−5035.
(48) Berthier, D. L.; Schmidt, I.; Fieber, W.; Schatz, C.; Furrer, A.; Wong, K.; Lecommandoux, S. Controlled Release of Volatile Fragrance Molecules from PEO-b-PPO-b-PEO Block Copolymer Micelles in Ethanol−Water Mixtures. *Langmuir* **2010**, *26*, 7953−7961.
(49) Penfold, J.; Thomas, R. K.; Bradbury, R.; Tucker, I.; Petkov, J. T.; Jones, C. W.; Webster, J. R. P. Probing the surface of aqueous surfactant-perfume mixed solutions during perfume evaporation. *Colloids Surf., A* **2017**, *520*, 178−183.
(50) Satari, B.; Karimi, K. Citrus processing wastes: Environmental impacts, recent advances, and future perspectives in total valorization. *Resour., Conserv. Recycl.* **2018**, *129*, 153−167.
(51) Parrino, F.; Fidalgo, A.; Palmisano, L.; Ilharco, L. M.; Pagliaro, M.; Ciriminna, R. Polymers of Limonene Oxide and Carbon Dioxide: Polycarbonates of the Solar Economy. *ACS Omega* **2018**, *3*, 4884−4890.
(52) Ciriminna, R.; Lomeli-Rodriguez, M.; Demma Carà, P.; Lopez-Sanchez, J. A.; Pagliaro, M. Limonene: a versatile chemical of the bioeconomy. *Chem. Commun.* **2014**, *50*, 15288−15296.
(53) Golmakani, M.-T.; Mendiola, J. A.; Rezaei, K.; Ibáñez, E. Pressurized limonene as an alternative bio-solvent for the extraction of lipids from marine microorganisms. *J. Supercrit. Fluids* **2014**, *92*, 1−7.
(54) Paggiola, G.; Stempvoort, S. V.; Bustamante, J.; Barbero, J. M. V.; Hunt, A. J.; Clark, J. H. Can bio-based chemicals meet demand? Global and regional case-study around citrus waste-derived limonene as a solvent for cleaning applications. *Biofuels, Bioprod. Biorefin.* **2016**, *10*, 686−698.
(55) Willrodt, C.; Halan, B.; Karthaus, L.; Rehdorf, J.; Julsing, M. K.; Buehler, K.; Schmid, A. Continuous multistep synthesis of perillic acid from limonene by catalytic biofilms under segmented flow. *Biotechnol. Bioeng.* **2017**, *114*, 281−290.
(56) Aissou, M.; Chemat-Djenni, Z.; Yara-Varón, E.; Fabiano-Tixier, A.-S.; Chemat, F. Limonene as an agro-chemical building block for the synthesis and extraction of bioactive compounds. *C. R. Chim.* **2017**, *20*, 346−358.
(57) Arrieta, M. P.; López, J.; Hernández, A.; Rayón, E. Ternary PLA−PHB−Limonene blends intended for biodegradable food packaging applications. *Eur. Polym. J.* **2014**, *50*, 255−270.
(58) Oberleitner, N.; Ressmann, A. K.; Bica, K.; Gärtner, P.; Fraaije, M. W.; Bornscheuer, U. T.; Rudroff, F.; Mihovilovic, M. D. From waste to value—direct utilization of limonene from orange peel in a biocatalytic cascade reaction towards chiral carvolactone. *Green Chem.* **2017**, *19*, 367−371.


DOI: 10.1021/acsomega.8b01858
*ACS Omega* 2018, 3, 15407−15415

(59) Nejad, E. H.; Paoniasari, A.; van Melis, C. G. W.; Koning, C. E.; Duchateau, R. Catalytic ring-opening copolymerization of limonene oxide and phthalic anhydride: Toward partially renewable polyesters. *Macromolecules* **2013**, *46*, 631−637.
(60) Firdaus, M.; Meier, M. A. R. Renewable polyamides and polyurethanes derived from limonene. *Green Chem.* **2013**, *15*, 370−380.
(61) Marcus, J.; Müller, M.; Nistler, J.; Touraud, D.; Kunz, W. Nano-droplet formation in water/ethanol or isopropanol/mosquito repellent formulations. *Colloids Surf., A* **2014**, *458*, 3−9.
(62) Drapeau, J.; Verdier, M.; Touraud, D.; Kröckel, U.; Geier, M.; Rose, A.; Kunz, W. Effective insect repellent formulation in both surfactantless and classical microemulsions with a long-lasting protection for human beings. *Chem. Biodiversity* **2009**, *6*, 934−947.
(63) Fiorito, S.; Taddeo, V. A.; Genovese, S.; Epifano, F. A green chemical synthesis of coumarin-3-carboxylic and cinnamic acids using crop-derived products and waste waters as solvents. *Tetrahedron Lett.* **2016**, *57*, 4795−4798.
(64) Lieutenant, K.; Lindner, P.; Gahler, R. A new design for the standard pinhole small-angle neutron scattering instrument D11. *J. Appl. Crystallogr.* **2007**, *40*, 1056−1063.
(65) Chiappisi, L. *The Structure of Limoncello*; Institut Laue−Langevin (ILL), 2016 DOI: 10.5291/ILL-DATA.INTER-372.
(66) Clará, R. A.; Marigliano, A. C. G.; Sólimo, H. N. Density, Viscosity, and Refractive Index in the Range (283.15 to 353.15) K and Vapor Pressure of $\alpha$-Pinene, d-Limonene, (±)-Linalool, and Citral Over the Pressure Range 1.0 kPa Atmospheric Pressure. *J. Chem. Eng. Data* **2009**, *54*, 1087−1090.



DOI: 10.1021/acsomega.8b01858
*ACS Omega* 2018, 3, 15407−15415